THE JOURNAL OF BIOLOGICAL CHEMISTRY VOL. 281, NO. 12, pp. 8233–8241, March 24, 2006

δ-Subunit Confers Novel Biophysical Features to αβγ-Human Epithelial Sodium Channel (ENaC) via a Physical Interaction*

Received for publication, November 16, 2005, and in revised form, January 10, 2006 Published, JBC Papers in Press, January 19, 2006, DOI 10.1074/jbc.M512293200

Hong-Long Ji[‡§1], Xue-Feng Su[§1], Shrestha Kedar[‡], Jie Li[‡], Pascal Barbry[¶], Peter R. Smith[§], Sadis Matalon[‡§], and Dale J. Benos[§2]

From the Departments of [‡]Anesthesiology and [§]Physiology and Biophysics, University of Alabama at Birmingham, Alabama 35205 and the [¶]Institut de Pharmacologie Moléculaire et Cellulaire, Centre National de la Recherche Scientifique UPR411, 06560 Sophia Antipolis, France

Native amiloride-sensitive Na^+ channels exhibit a variety of biophysical properties, including variable sensitivities to amiloride, different ion selectivities, and diverse unitary conductances. The molecular basis of these differences has not been elucidated. We tested the hypothesis that co-expression of δ-epithelial sodium channel (ENaC) underlies, at least in part, the multiplicity of amiloride-sensitive Na^+ conductances in epithelial cells. For example, the δ-subunit may form multimeric channels with αβγ-ENaC. Reverse transcription-PCR revealed that δ-ENaC is co-expressed with αβγ-subunits in cultured human lung (H441 and A549), pancreatic (CFPAC), and colonic epithelial cells (Caco-2). Indirect immunofluorescence microscopy revealed that δ-ENaC is co-expressed with α-, β-, and γ-ENaC in H441 cells at the protein level. Measurement of current-voltage relationships revealed that the cation selectivity ratios for $Na^+/Li^+/K^+/Cs^+/Ca^{2+}/Mg^{2+}$, the apparent dissociation constant (K_i) for amiloride, and unitary conductances for δαβγ-ENaC differed from those of both αβγ- and δβγ-ENaC ($n = 6$). The contribution of the δ subunit to P_{Li}/P_{Na} ratio and unitary Na^+ conductance under bi-ionic conditions depended on the injected cRNA concentration. In addition, the EC_{50} for proton activation, mean open and closed times, and the self-inhibition time of δαβγ-ENaC differed from those of αβγ- and δβγ-ENaC. Co-immunoprecipitation of δ-ENaC with α- and γ-subunits in H441 and transfected COS-7 cells suggests an interaction among these proteins. We, therefore, concluded that the interactions of δ-ENaC with other subunits could account for heterogeneity of native epithelial channels.

The diverse biophysical properties of native epithelial Na^+ channels have been reviewed previously (1). Na^+ conductance, P_{Na}/P_K, and amiloride affinity differ between various tissues and species. For example, a 10-pS amiloride-sensitive Li^+ conductance was recorded in H441 cells, and two amiloride-sensitive conductances (4 and 20 pS) were found in A549 cells (2, 3). Additional native amiloride-sensitive channels with different single channel conductances have been reported (4). Generally, native epithelial Na^+ channels can be classified into three subtypes according to their permeability to cations (1, 5). The highly Na^+ selective channel (type I) resembles αβγ-ENaC[3] heterologously expressed in oocytes. However, the molecular basis of the moderate selective (type II) and nonselective Na^+ channels (type III) in epithelia, such as the 20-pS channels in A549 (6) and 10-pS channel in H441 cells (2), is unknown.

The α-ENaC subunit was originally cloned from the rat colon and has subsequently been identified in a variety of mammalian and amphibian species (1, 7). Five ENaC subunits have been cloned to date, namely α-, β-, γ-, δ-, and ε-ENaC. Among them, the β- and γ-subunits regulate the channel activity of the "conducting" α-, δ-, and ε-ENaC subunits when heterologously expressed in oocytes and cell lines (7). Biophysical characterization of αβγ-ENaC channels has revealed a Na^+ conductance of 4 pS and a Li^+ conductance of 7 pS, respectively. αβγ-ENaC is highly permeable to Na^+ but virtually impermeable to K^+, with a P_{Na}/P_K greater than 20. Amiloride sensitivity and other properties of αβγ-ENaC are reflective of the characterization of highly Na^+ selective channels in native epithelial cells. In comparison with the α-subunit, δ-ENaC exhibits differences in Na^+ conductance, amiloride affinity, self-inhibition, and P_{Na}/P_{Li} selectivity ratio (8–11). However, neither αβγ- nor δβγ-ENaC can match all native amiloride-sensitive Na^+ channels in their biophysical properties. Additionally, many of the cloned, conductive ENaC subunits are not activated by cAMP-elevating agents, which is a hallmark of native epithelial Na^+ channels.

The biophysical properties of ENaC depend on channel composition. α-like conducting subunits can form a channel sharing identical properties to channels composed of α-like and βγ subunits (9, 10, 12, 13). In contrast, αβ- and αγ-ENaC channels display variant amiloride sensitivity, conductance, and Na^+ permeability (14, 15). On the other hand, properties of native amiloride-sensitive Na^+ channels are dependent on culture conditions (16, 17). Cells grown on permeable supports have a channel that more closely resembles heterologously expressed αβγ-ENaC channels than the channels expressed by cells grown on coverslips (18). Although it has been reported that a functional ENaC complex is composed of either $2\alpha/1\beta/1\gamma$, or alternatively, $3\alpha3\beta/3\gamma$ (7, 19), channel properties may not be determined in a stoichiometric manner.

The existence of other subunits may play an important role in determining native channel properties. Indeed, numerous studies demonstrated that culture conditions, cellular protein polarization, subunit composition, and splice variants can partly account for the diversity in channel properties (1, 16, 17). However, the putative influence of the δ-subunit co-expression on the ENaC channel properties has not been documented. In the present study, we have tested the hypothesis that δ-ENaC is co-expressed with αβγ-ENaC subunits in epithelia and that δ-ENaC influences the biophysical features of αβγ channels when co-expressed in oocytes. Our results indicated that monovalent and divalent cation selectivities, single channel Na^+ conductance, amiloride affinity, gating kinetics, and proton activation of δαβγ-hENaC were intrinsically distinguishable from those of αβγ- and δβγ-ENaC. We

* The work was supported by Cystic Fibrosis Foundation Grants JI04G0, DK37206, DK56596, HL075540, and HL51173. The costs of publication of this article were defrayed in part by the payment of page charges. This article must therefore be hereby marked "*advertisement*" in accordance with 18 U.S.C. Section 1734 solely to indicate this fact.

[1] Both authors equally contributed to the study.

[2] To whom correspondence should be addressed: Dept. of Physiology and Biophysics, University of Alabama at Birmingham, 1918 University Blvd., 704 MCLM, Birmingham, AL 35294-0005. Fax: 205-934-2377; E-mail: benos@physiology.uab.edu.

[3] The abbreviations used are: ENaC, epithelial sodium channel; hENac, human ENaC; MES, 2-morpholinoethanesulfonic acid; RT, reverse transcription; HA, influenza A virus hemagglutinin; MOT, mean open time; MCT, mean closed time; CFPAC, human pancreatic duct cells; PBS, phosphate-buffered saline; pS, picosiemens.

also demonstrated the presence of δ-ENaC mRNA in human lung, pancreatic, and colonic epithelial cells using RT-PCR. Also, for the first time, we showed that native α- and γ-ENaC co-immunoprecipitate with δ-ENaC in H441 cells and in transiently transfected COS-7 cells, supporting the idea that these four mammalian ENaC subunits combine to form multimeric channels with novel biophysical properties.

MATERIALS AND METHODS

Oocyte Expression and Whole-cell Recordings— cRNAs for human δ-, α-, β-, and γ-ENaC (hENaC) were prepared as described previously (20). Defolliculated oocytes were cytosolically injected with hENaC cRNAs (25 ng) per oocyte in 50 nl of RNase free water with a ratio of 1δ:1α:1β:1γ subunit (except for cRNA concentration-dependent experiments) and incubated in half-strength L-15 medium. Whole-cell cation currents were measured by the two-electrode voltage clamp technique 2 days after injection. Oocytes were impaled with two electrodes, each having resistances of 0.5–2 megaohms when filled with 3 M KCl. A TEV 200 voltage clamp amplifier was used to clamp the oocytes with concomitant recording of currents. Two reference electrodes were connected to the bath. Sampling protocols were generated by pCLAMP 8.0, and the current at −60 mV was simultaneously monitored with a chart recorder. The control superfusate was ND-96 (in mM: 96 NaCl, 1 $MgCl_2$, 1.8 $CaCl_2$, 2 KCl, and 5 HEPES, pH 7.5). Superfusate with pH 6 or below was buffered with MES. pH was adjusted with NaOH and HCl. In experiments designed to measure the ion selectivity, Na^+ salt was replaced with equal molar amounts of Li^+, K^+, Cs^+, Ca^{2+}, and Mg^{2+} for determination of ion selectivity. Switching of bath solutions with neutral or acidic pH was controlled by an SF-77B Perfusion Fast-Step system (Warner Instrument Corp., Hamden, CT). Current-voltage relationships were acquired by stepping the holding potential in 20-mV increments from −120 to +80 mV after the monitoring currents were stable, with and without the application of amiloride (100 μM). Data were sampled at a rate of 1 kHz and filtered at 500 kHz.

Reverse Transcription-PCR—Confluent H441, A549, CFPAC, and Caco-2 cells were scraped into ice-cold PBS. Following pelleting in a microcentrifuge, the PBS was discarded, and the cells were snap-frozen in a dry ice-methanol mixture and stored at −80 °C. Total RNA was extracted using TRIzol reagent (Invitrogen) according to the manufacturer's instructions. RNA was dissolved in RNase-free water and stored at −80 °C. RNA concentration was assessed by spectrophotometry at 260 nm. RNA quality was confirmed by running 5 μg of total RNA from each preparation on a 1.2% denatured agarose gel. The specific oligonucleotide primers for the RT-PCR analysis of the α-, β-, δ-, and γ-ENaC subunits were as follows: α-ENaC, 5′-AAC AAA TCG GAC TGC TTC TAC-3′ (sense), 5′-AGC CAC CAT CAT CCA TAA A-3′(antisense); β-ENaC, 5′-GGG ACC AAA GCA CCA AT-3′ (sense), 5′-CAG ACG CAG GGA GTC ATAG-3′ (antisense); δ-ENaC, 5′-CGA AGC ATG GAC GGG AGA ATG-3′ (sense), 5′-GGT GCC AGT GAC GCT CAA AGA-3′ (antisense); γ-ENaC, 5′-GCA CCG TTC GCC ACC TTC TA-3′ (sense), 5′-AGG TCA CCA GCA GCT CCT CA-3′ (antisense). Sequence accession numbers in GenBank™ are 38197484, 4506816, 34101281, and 42476332 for the α-, β-, δ-, and γ-subunits, respectively. The corresponding product sizes are 406 bp (α), 440 bp (β), 325 bp (δ), and 456 bp (γ). Custom primers specific for δ-, α-, β-, and γ-ENaC were synthesized by Sigma Genosys and used at a final concentration of 0.4 μM. RT-PCR was performed using the OneStep RT-PCR kit (Qiagen) in a Mastercycler gradient thermocycler (Eppendorf Scientific). One microgram of total RNA was added as a template for each reaction. Reverse transcription was carried out using a single cycle of 50 °C for 30 min. This was followed by a single cycle of 95 °C for 15 min to inactivate the reverse transcriptase while activating the HotStart TaqDNA polymerase, and then 30 cycles of 94 °C for 0.5 min, 56 °C for 1 min, 72 °C for 1.5 min were performed followed by a single 10-min cycle at 72 °C for extension. RT-PCR products were electrophoresed on a 2% agarose gel using 100-bp PCR markers (Promega) as a standard to determine the molecular size. Products of the predicted molecular size were excised and purified from the gel using the QIAquick gel extraction kit (Qiagen) and subcloned into the pCR-2.1 vector (Invitrogen). Positive clones were selected by blue/white screening and followed by digestion with EcoRI (Promega) to verify incorporation of insert of the correct size. Authenticity of PCR products in the pCR2.1 vector were verified by automated DNA sequencing (DNA Sequencing Facility, Iowa State University).

Immunofluorescence Microscopy—Confluent H441 cell monolayers were grown on 12-mm diameter polycarbonate filters (Corning Costar) for approximately 2 weeks. Following fixation in 3% buffered formaldehyde for 20 min, cells were permeabilized in 0.01% Triton X-100 in PBS for 5 min, and nonspecific protein binding sites were blocked using 5% bovine serum albumin in PBS for 30 min. Anti-δENaC (Open Biosystems, Huntsville AL) as well as α-, β-, and γ-ENaC polyclonal antibodies (prepared by Pascal Barbry) at 5–20 μg/ml for 2 h at room temperature) was used to detect ENaC protein. An 18-amino acid peptide in extracellular loop (RESAFKLSTGTSRWPSAK) was antigen for δ-ENaC antibody preparation. Cells incubated with PBS in the absence of ENaC antibodies serve as control. Nuclei were stained with Vectashield-4′,6-diamidino-2-phenylindole (Vector Labs). Images were captured on an Olympus IX170 inverted epifluorescence microscope using SenSys-cooled charge-coupled high resolution camera (Photometrics, Tucson, AZ). Images were assembled using Adobe PhotoShop.

Co-immunoprecipitation—COS-7 or H441 cells were grown in low bicarbonate Dulbecco's modified Eagle's medium supplemented with 10% fetal bovine serum and penicillin-streptomycin. Cells were maintained at 37 °C and 5% CO_2. COS-7 cells were plated at a density of 2.4×10^6 cells in 100-mm plates 24 h prior to transfection. Cells were transfected with ~24 μg of each cDNA construct or vector alone using Lipofectamine 2000 (Invitrogen) following the manufacturer's instructions. COS-7 and H441 cells were lysed in a lysis buffer (in mM: 120 NaCl, 100 KCl, 20 EDTA, 1 dithiothreitol, 20 Tris-HCl, 1% Triton X-100, pH 7.5) supplemented with one protease inhibitor mixture tablet (Roche Applied Science)/10 ml of lysis buffer at 4 °C for 1 h. The lysate was centrifuged at 14,000 rpm for 10 min, and the pellet was discarded. The supernatant was incubated with 10 μg of anti-αENaC (Affinity Bioreagents) or anti-HA antibody (Sigma) to immunoprecipitate the specific proteins for 2 h at 4 °C. The supernatant of H441 cell lysates was incubated with 10 μg of anti-αENaC (Affinity Bioreagents) or anti-δENaC antibody (Open Biosystems) to immunoprecipitate the specific proteins for 2 h at 4 °C. Subsequently, 50 μl of protein A/G-plus Agarose beads was added and incubated for 1 h at 4 °C. The beads were washed for five times with the lysis buffer, resuspended in 2× SDS sample buffer, and boiled at 95 °C for 5 min. The samples were analyzed by Western blotting (8% SDS-PAGE gel) using anti-HA monoclonal (Sigma), anti-γENaC (Affinity Bioreagents), and anti-αENaC polyclonal antibodies (Affinity Bioreagents).

Single Channel Patch Clamp Assay—Unitary Na^+ and Li^+ conductance in oocytes was digitized from on-cell and inside-out patches isolated from vitelline membrane-stripped eggs as described previously (21). Linear regression analysis was applied to the single channel current-voltage curves to compute the slope conductance.

Data Analysis—Data were primarily analyzed with the Axon Clampfit 9.2 and further statistically computed and plotted with Origin 7.5

(OriginLab). Proton-activated Na^+ current at each pH was computed by subtracting the basal current from the peak current in the presence of protons. The EC_{50} of external pH was calculated by fitting the acid-activated current with the Hill equation

$$I_{Na} = I_{max} \frac{pH_o^n}{pH_o^n + EC_{50}^n} \quad \text{(Eq. 1)}$$

where I_{Na} is the proton-activated currents, I_{max} is the maximal acid-activated current, pH_o stands for the extraoocyte pH, EC_{50} represents the value of pH_o that results in half of the maximal current of the ENaC channel, and n is the Hill coefficient.

Mean open time (MOT) and mean closed time (MCT) were calculated using the equations

$$MOT = \frac{T \cdot NP_o}{e/2} \quad \text{(Eq. 2)}$$

and

$$T_c = \frac{NT}{e/2} - MOT \quad \text{(Eq. 3)}$$

where T is the total recording time, e is the event number, and NP_o have their usual meanings (22, 23). Because the heterologously expressed ENaC in oocytes exhibit multiple channels in each patch, the real baseline at which all of channels are silent is difficult to identify; therefore, the values of MOT and MCT were calculated based on the assumption that the lowest level during the recording period represents the closed level.

All results are presented as mean ± S.E. of amiloride-sensitive currents. Amiloride-sensitive currents are defined as the difference between the total current and the amiloride-resistant current. One-way analysis of variance computation combined with the Bonferroni test was used to analyze data with unequal variance between each group. A probability level of 0.05 was considered significant.

RESULTS

Expression of ENaC mRNA in Human Epithelia—To examine whether δ-ENaC is co-expressed with the αβγ-subunits in human epithelial cells at the mRNA level, cells that have previously been shown to have an functional amiloride-sensitive Na^+ conductance were chosen for RT-PCR. As shown in Fig. 1, a 419-bp product was detected in human lung epithelial cells (H441), human pancreatic epithelial cells (CFPAC), human colonic epithelial cells (Caco-2), and human lung epithelial cells (A549). Sequencing of this product from each cell line indicated that the band corresponded to δ-ENaC originally cloned from human testis (GI 21752051), encoding a 714-amino acid protein. An additional 325-bp product was also present in A549, CFPAC, and Caco-2 but not H441 cells. Sequencing of this product revealed that it corresponds to a δ-ENaC isoform (GI34101282) initially cloned from human renal epithelia (9), which encodes a protein of 638-amino acid residues. Expression of α- and γ-ENaC was also detected in these four human epithelial cells, whereas the β-subunit was only weakly expressed in Caco-2 cells and was absent in CFPAC cells (Fig. 1).

Expression of δ-ENaC Protein in Lung Epithelial Cells—To detect δ-ENaC expression at the protein level, H441 monolayers grown on filters were immunostained with a specific anti-δ-ENaC antibody followed by a fluorescein isothiocyanate-conjugated secondary antibody. δ-ENaC expression was observed (Fig. 2). α-, β-, and γ-ENaC expression were also detected in H441 monolayers, in agreement with other studies (2, 24). Cells incubated with nonimmune IgG and the secondary antibody did not exhibit immunofluorescence. Differences in fluorescence intensity may reflect variable ENaC subunit expression at the protein level and different affinity among antibodies against ENaC proteins. Similar results were seen in A549 cells. These results suggest that δ-ENaC is co-expressed with α-, β-, and γ-ENaC protein in native human lung epithelial cells.

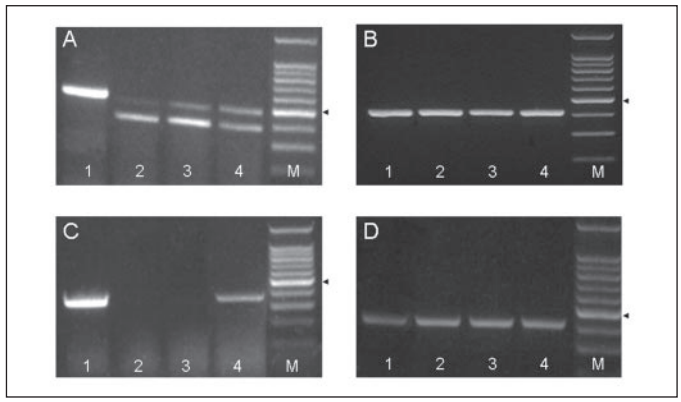

FIGURE 1. **Reverse transcription-PCR analysis of δ-, α-, β-, and γ-ENaC mRNA expression in human epithelial cell lines.** The expression pattern of ENaC subunits was confirmed with 2–3 independent experiments using the OneStep RT-PCR kit. For each cell line, the same passage of cells was used to detect δ- (*A*), α- (*B*), β- (*C*), and γ-ENaC (*D*) mRNA expression. The lanes from *left* to *right* represent human lung epithelial cells-H441 (*1*), human pancreatic epithelial cells-CFPAC (*2*), human colonic epithelial cells-Caco-2 (*3*), human lung epithelial cells-A549 (4), and markers (*M*). The *arrows* indicate a 500-bp marker.

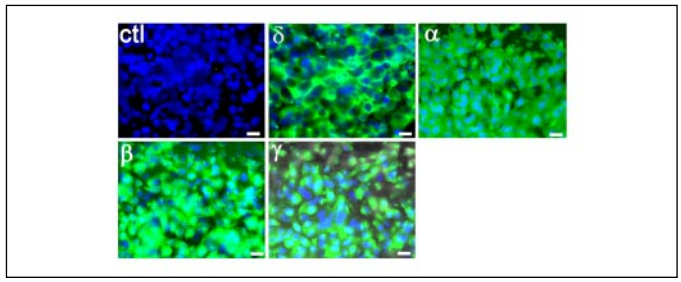

FIGURE 2. **Indirect immunofluorescent detection of ENaC in H441 cells.** Confluent H441 cells were incubated with specific antibodies against δ-, α-, β-, and γ-ENaC subunits. ENaC protein was detected (*green channel*) with fluorescein isothiocyanate-conjugated secondary antibodies. Nonimmune IgG was used to as negative control (*ctl*). Cell nuclei were stained with Hoechst Dye (*blue channel*). the *bar* equals 20 μm; $n = 3$.

Co-immunoprecipitation of α- and γ-ENaC with δ-ENaC in H441 and COS-7 Cells—Co-expression of δ-ENaC with α-, β-, and γ-ENaC indicated that these four ENaC subunits may associate with each other to form a multiple subunit channel protein complex. To test this hypothesis, we first detected native δ-ENaC protein expression in H441 cells. As shown in Fig. 3*A* and in the *right lane* in Fig. 3*C*, δ-, α-, and γ-ENaC proteins were detected as 85–90 kb for δ- and α-ENaC and 150 kb for γ-ENaC. γ-ENaC was found to co-immunoprecipitate with δ- and α-ENaC (Fig. 3*B*). Specificity was demonstrated by Western analysis with anti-γENaC following pretreatment of the anti-γENaC antibody with excess neutralizing peptide (Fig. 3*B*). In addition, δ-ENaC also precipitated with α-subunit in H441 cells (Fig. 3*C*) and in COS-7 cells following transient transfection of HA-tagged δ-ENaC and α-ENaC.

Cation Permeability—In this set of experiments, we tested the hypothesis that co-expression of δ-ENaC alters the ion selectivity of αβγ-ENaC. As shown in Fig. 3*A*, the inward amiloride-sensitive Na^+ current was greater than that carried by Li^+ ions. Much less inward and relative greater outward currents were detected when K^+, Cs^+, Ca^{2+},

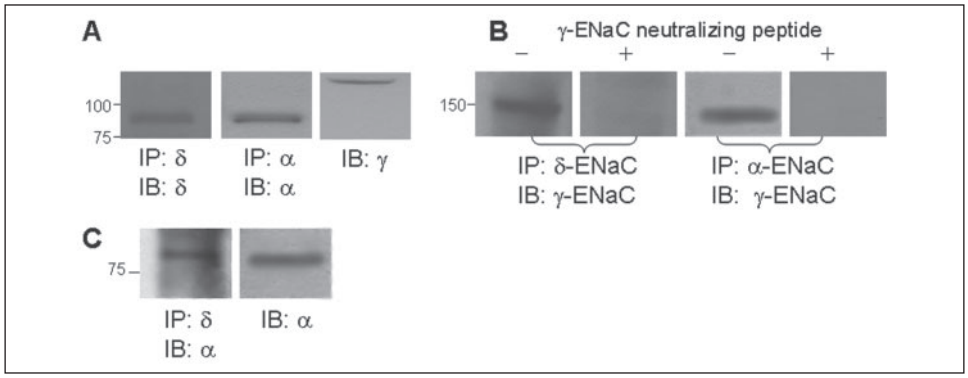

FIGURE 3. **Co-immunoprecipitation of δ- and α- or δ- and γ-ENaC subunits from H441 cells.** *A*, expression of δ-, α-, and γ-ENaC. δ-, γ-, and α-ENaC proteins (50 μg/lane) were detected by immunoprecipitation (*IP*) followed by immunoblotting (*IB*) with the appropriate antibodies. Five μl of serum for δ-ENaC antibody or 1 μg/ml for α and γ-ENaC antibodies was used for both immunoprecipitation and immunoblotting. *B*, co-immunoprecipitation of γ- with δ-ENaC, and γ- with α-ENaC. γ-ENaC was detected by immunoblotting with γ-ENaC antibody on proteins co-immunoprecipitated with both δ- and α-ENaC antibodies. The specificity of γ-ENaC signal was established by the lack of signal when immunoblotting was performed in the presence of immunogenic peptide (neutralizing peptide,1 μg/ml). *C*, co-immunoprecipitation of δ- with α-ENaC. Cell lysates were immunoprecipitated using a specific antibody against δ-ENaC, and immunoblots of the precipitated proteins were probed with α-ENaC antibody. As a control, an aliquot of the H441 cell lysates was also probed with α-ENaC antibody without precipitation of δ-ENaC antibody. These experiments were repeated three times with identical results.

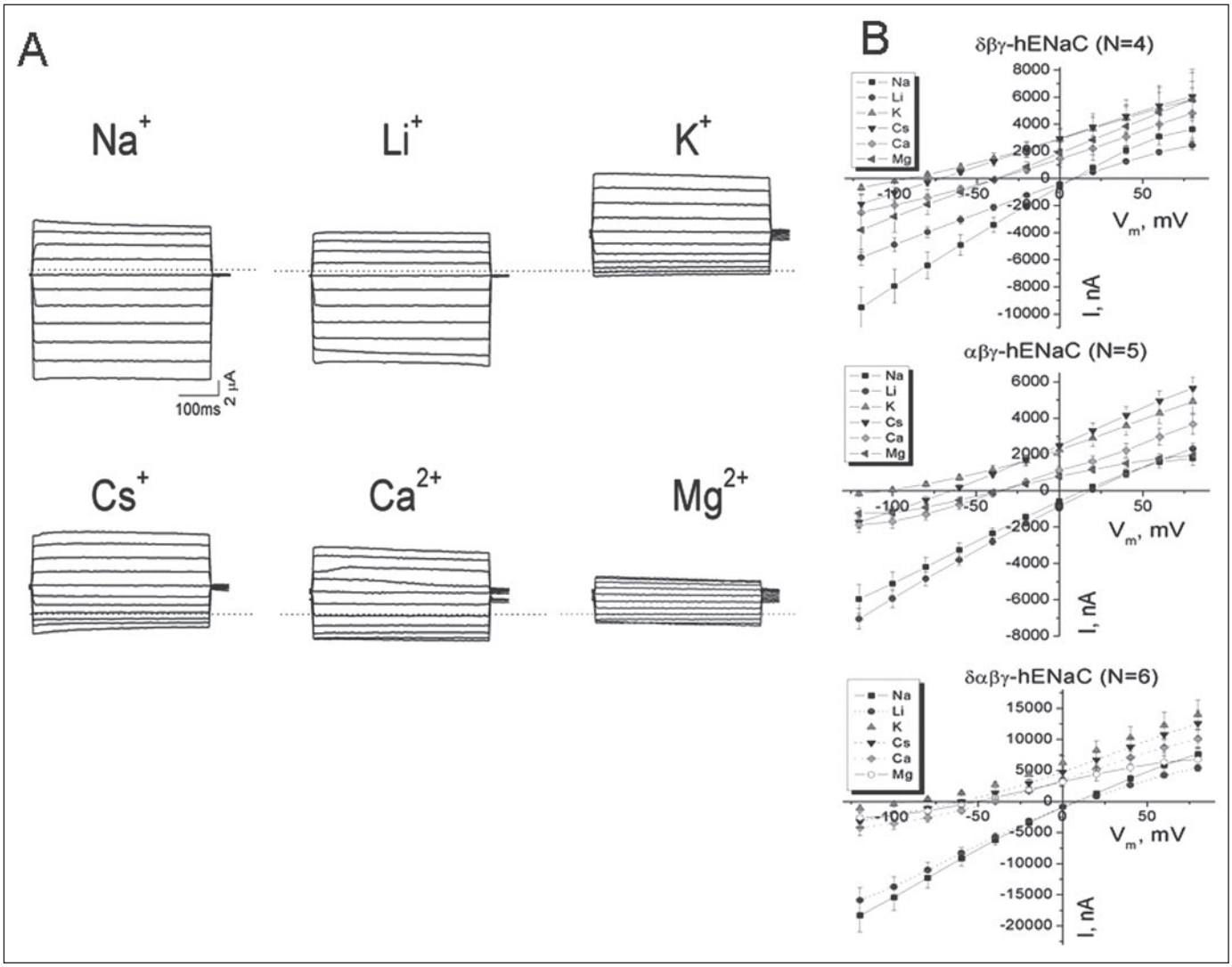

FIGURE 4. **Cation selectivity of δαβγ-hENaC expressed in oocytes.** *A*, representative amiloride-sensitive whole-cell current traces recorded from an oocyte expressing δαβγ-hENaC. Oocytes were initially perfused with ND-96 medium (96 mM Na^+), and step I-V traces were obtained. Oocytes were hold at stepped voltages from −120 mV to +80 mV in 20-mV increments. Amiloride-sensitive traces were computed as the difference between the currents with and without 100 μM amiloride in the bath. The bath solution was switched to media in which the sodium was substituted with equamolar monovalent or divalent cations. The *dashed lines* indicate zero current level. $n = 4–6$. *B*, cation permeation of δβγ-, αβγ-, and δαβγ-hENaC. Whole-cell amiloride-sensitive currents (I) at membrane potential (V_m) from −120 mV to +80 mV were recorded from oocytes expressing δβγ- (*top*), αβγ- (*middle*), and δαβγ-hENaC (*bottom*). The I-V curves were fitted with the Goldman-Hodgkin-Katz current equation to calculate the absolute permeability to each cation and relative ratios to sodium.

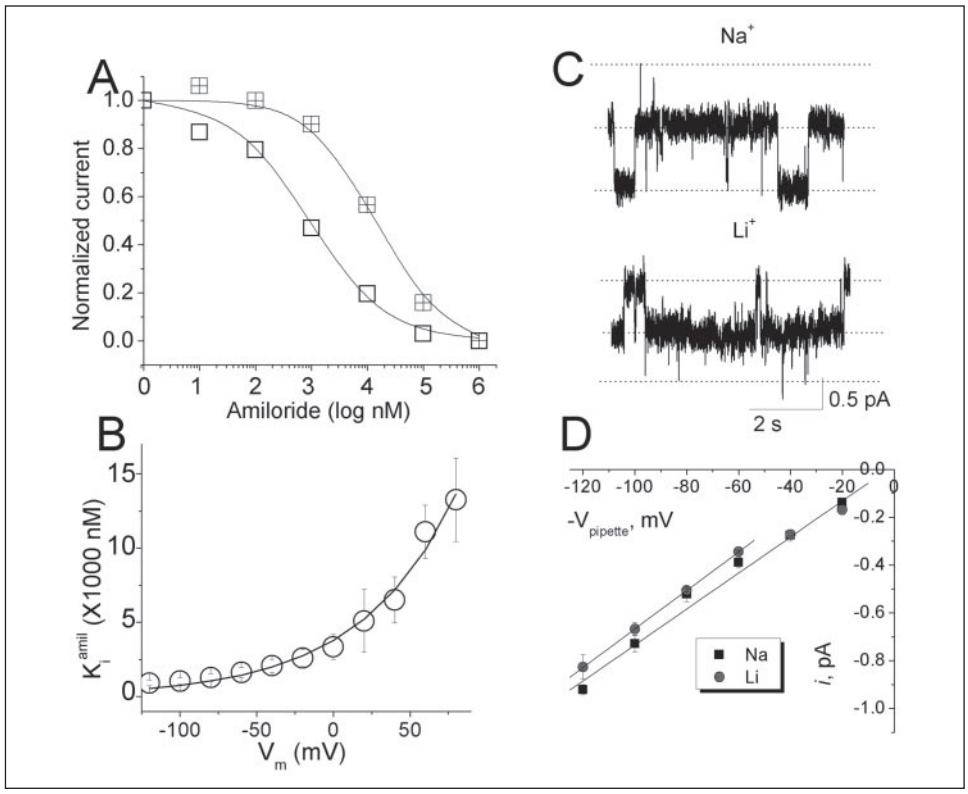

FIGURE 5. **Amiloride sensitivity and unitary conductances of δαβγ-hENaC.** *A,* dose-response curves were plotted with normalized amiloride-sensitive Na^+ currents as a function of amiloride concentration at −120 mV (*open square*) and +80 mV (*open square with cross*). The apparent dissociation constant of amiloride (K_i^{amil}) was computed by fitting the dose-response curve with the Hill equation. *B,* voltage dependence of amiloride blockade. The voltage-sensitive fractional distance for amiloride is 0.41, between α- (0.34) and δ-ENaC (0.48). *C,* single channel Na^+ and Li^+ current traces. Representative single channel traces digitized at −120 mV. Cell-attached patches were used with either 100 mM Na^+ or 100 mM Li^+ in the pipette and bath solutions. The *dotted lines* show opening levels. The real closing level (base line) was unknown during a 5-min recording period. These are segments. *D,* unitary current-voltage curves. The unitary Na^+ conductance is 8 ± 0.2 pS ($n = 6$), different from those of αβγ- (4 pS) and δβγ-hENaC (12 pS) (21).

and Mg^{2+} were used as charge carriers. Meanwhile, the reversal potential shifted leftward from depolarization voltages (10–20 mV) by ~50–150 mV. Additionally, the resting membrane potentials, which were generally above 0 mV under current clamp configuration in oocytes perfused with Na^+ (or Li^+), showed hyperpolarization to a variable extent (Fig. 3*A*).

To calculate the permeability ratios between Na^+ and the other cations, amiloride-sensitive current-voltage curves were fitted with the Goldman-Hodgkin-Katz current equation as described previously (Fig. 3*B*) (20). The P_X/P_{Na} ratios of $Na^+/Li^+/K^+/Cs^+/Ca^{2+}/Mg^{2+}$ were 1/**0.6**/0.07/0.2/0.26/0.4 for δβγ-ENaC. However, they were 1/**1.2**/0.02/0.29/0.31/0.21 for αβγ-ENaC and 1/**0.88**/0.02/0.14/0.23/0.14 for δαβγ-hENaC, respectively. Our results of wild type αβγ- and δβγ-ENaC are consistent with previously published observations (8, 9, 25). In particular, the normalized permeability to Li^+ (P_{Na} is 1.0) for δαβγ-ENaC was 0.88, which was distinguishable from those of αβγ- (1.2) and δβγ-ENaC (0.6). Significant differences in normalized permeabilities to the other monovalent and divalent cations was not observed between αβγ-, δβγ-, and δαβγ-ENaC channels, as shown in Fig. 4.

Amiloride Sensitivity—The K_i of amiloride for δβγ-ENaC is in the micromolar range (*versus* <100 nM for αβγ-ENaC). Amiloride blocking of δβγ-ENaC is much more voltage-dependent when compared with the αβγ channel (21). To determine amiloride sensitivity of δαβγ-ENaC, we perfused oocytes with solutions containing 1 nM, 10 nM, 100 nM, 1 μM, 10 μM, 100 μM, and 1 mM amiloride at holding potentials ranging from −120 mV to +80 mV. Fig. 5 shows that the dose-response curves shifted rightward at depolarized potentials. The K_i of amiloride at −120 mV was 920 ± 185 nM and 13746 ± 2805 nM at +80 mV, respectively, which significantly differ from those of αβγ-ENaC ($p < 0.05$, $n = 6$).

To further investigate the voltage dependence of amiloride inhibition for δαβγ-hENaC, the values for K_i^{amil} were plotted against the applied membrane potentials (Fig. 5*B*). The more depolarizing the membrane potential, the greater the value of K_i^{amil}. As we have previously described for αβγ- and δβγ-ENaC, positively charged amiloride interacts with ENaC in a voltage-dependent manner (21). The K_i of amiloride at 0 mV estimated by fitting the voltage-dependent plot with the Woodhill equation was 3.79 ± 0.2 μM for δαβγ-ENaC, whereas it was 13.1 and 0.33 μM for δβγ- and αβγ-ENaC, respectively (21). The voltage-sensitive fractional distance for amiloride was 0.41. In comparison, it was 0.34 for αβγ-ENaC and 0.48 for δβγ-ENaC, respectively (21).

Unitary Conductance—Because the ion permeability ratio (P_{Na}/P_{Li}) and apparent equivalent dissociation constant of amiloride for the δαβγ-ENaC channel are the arithmetic mean of those of αβγ- and δβγ-ENaC, the question arose whether oocytes injected with δαβγ-ENaC subunits express two separate populations of ENaC, that is, αβγ- and δβγ-ENaC channels or one population of δαβγ-channels with novel biophysical characteristics. To address this question, on-cell patches were used to measure single channel conductances (Fig. 6*C*). Only one unitary Na^+ or Li^+ current level was observed (Fig. 5*D*), and the corresponding slope conductances, respectively, were 8 ± 0.2 pS for Na^+ and 7.5 ± 0.1 pS for Li^+ ($n = 6$). No amiloride-sensitive subconductance was observed.

Gating Kinetics—We measured the MOT and MCT for δαβγ-ENaC (Fig. 6). As shown in Fig. 6, the MOT and MCT for δαβγ-ENaC were significantly less than the corresponding values for αβγ- and δβγ-ENaC. The MOT values for αβγ- and δβγ-ENaC were greater than that of δαβγ-ENaC ($p < 0.05$). In addition, the MCT values of αβγ-ENaC were almost 10-fold of that for δαβγ-ENaC ($p < 0.05$).

Proton Activation—Recently, we found that δβγ-ENaC, but not αβγ-ENaC, was activated by extracellular protons (25). To test the pH sensitivity of δαβγ-ENaC, oocytes were perfused with bath solutions with neutral or acidic pH. Similar to the δβγ-ENaC channel expressed in oocytes, the inward current of δαβγ-ENaC was activated by extra-oocyte acidic pH in a concentration-dependent pattern (Fig. 7). The pH value required for half-activation of the maximal pH-activated current

level (EC_{50}) was 6.5 ± 0.1 (n = 8). This differs from pH 6.0 for δβγ-ENaC (25).

Self-inhibition—Self-inhibition by extracellular Na^+ ions is a biophysical hallmark of the ENaC channels (1). To characterize this inherent biophysical property, the self-inhibition time of Na^+ for δαβγ-ENaC was examined (Fig. 8). To calculate self-inhibition time, the currents at −60 mV were digitized while switching bath solutions from low Na^+ ND-96 medium (1 mM Na^+) to ND-96 (96 mM Na^+) medium. The current fraction from the time point for the first time to switch bath solution (from 1 to 100 mM) to the peak of current and from the peak of current to the time point for the second time to switch bath solution (from 100 to 1 mM) was fitted with the first-order exponential function for estimating τ_a and τ_{si}, respectively (Fig. 8).

Fig. 9 shows that the inward current reached its peak in less than 1 s followed by a run-down in the presence of constant external Na^+ level. The self-inhibition time (τ_{si}) for δαβγ-ENaC was 3427 ± 217 ms (n = 13), which was significantly greater than that of αβγ-ENaC (2584 ± 72 ms, n = 47, $p < 0.05$) but less than that of δβγ-ENaC (8626 ± 1541 ms, n = 23, $p < 0.01$). In contrast, the activation (τ_a) was not changed significantly. The αβγ-ENaC current displayed a steep run-down (45% of the peak current in 12.5 s), whereas the δβγ-ENaC current level decreased to a lesser extent (12% of peak current in 12.5 s). These results are consistent with measurements of rat and mouse αβγ-ENaC expressed in oocytes (26, 27). Therefore, the corresponding ratio of the peak and sustained currents was much less for αβγ-ENAC when compared with those of δβγ and δαβγ-ENaC ($p < 0.01$).

Dependence of P_{NA}/P_{Li} Ratio and Unitary Na^+ Conductance on Injected cRNA Concentrations—To determine the expression level of δ-ENaC needed to confer the biophysical features of αβγ-ENaC, we measured the P_{Li}/P_{Na} ratios and unitary Na^+ conductance in oocytes co-injected with various ratios of δ- and αβγ-ENaC cRNAs (Fig. 9). The P_{Li}/P_{Na} ratio (*left panel*) in oocytes co-injected with an equivalent concentration (1δ:1α) of δ- and α-ENaC cRNAs was significantly lower when compared with that of αβγ-ENaC (0.7 *versus* 2.0, $p < 0.05$). Even with the cRNA ratio of 1δ:10α, the relative Li^+ permeability reduced markedly. Meanwhile, the unitary Na^+ conductance increased in one-third of patches in oocytes expressing 1δ:10α-ENaC (*right panel*). A further increase (10δ:1α) in the δ-subunit cRNA co-injected elevated the conductance closing to the level of δβγ-ENaC.

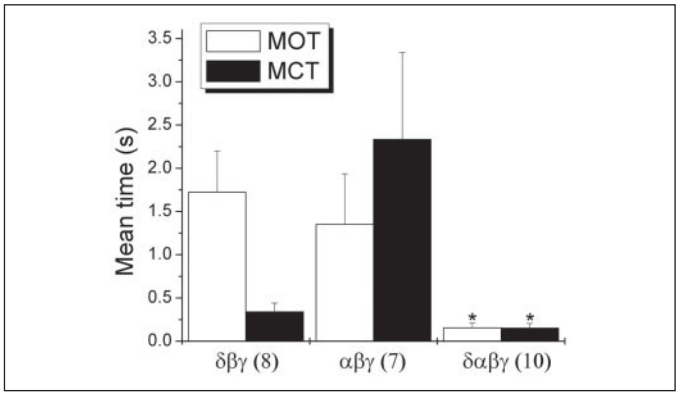

FIGURE 6. **MOT and MCT of δαβγ-hENaC.** The MOT and MCT values were calculated based on the assumption that the lowest level during the recording period was closed level. Single channel Na^+ traces at −120 mV were obtained from cell-attached patches. The *numbers in brackets* are patches analyzed. *, $p < 0.05$ when compared with αβγ- or δβγ-hENaC.

DISCUSSION

The aim of the present study was to test the hypothesis that the δ-ENaC subunit may combine with αβγ-subunits to form a channel complex exhibiting unique biophysical properties. δαβγ-hENaC heterologously expressed in oocytes was characterized by ion selectivity, amiloride sensitivity, unitary Na^+ conductance, gating kinetics, proton activation, and self-inhibition that differed from those of both αβγ- and δβγ-hENaC. We have provided evidence for the presence of δ-, α-, β-, and γ-ENaC mRNA and protein in human pulmonary epithelial cells (H441 and A549). Our immunocytochemical and co-immunoprecipitation data from H441 cells suggest that the ENaC channel complex in native epithelial cells may be maximally composed of all four mammalian ENaC subunits.

Transcripts for α-, β-, and/or γ-ENaC subunits have been detected in untreated and dexamethasone-treated H441 (2, 28–30) and A549 cells (2, 6, 24, 31) by RT-PCR, Northern blot, and ribonuclease protection assays. Expression of α-, β-, and γ-ENaC in human lung epithelial cells reported in the present study agreed with these observations. Furthermore, an amiloride-sensitive channel has been identified in H441 and A549 cells using patch clamp and Ussing chamber techniques by several groups (2, 3, 6, 28, 31–33). This is the first report of ENaC mRNA expression in Caco-2 cells, although a benzamil-sensitive short circuit current has been reported (34, 35). A novel finding of this study was that the δ-subunit is co-expressed with α-, β-, and γ-ENaC in the native human epithelial cells we examined. Consistent with the previous reports of human α- and δ-ENaC transcripts in pancreatic cells (9, 10), α- and δ-ENaC transcripts were detected in CFPAC cells. However, a functional amiloride-sensitive conductance has not been successfully detected in rat, bovine, or human pancreatic duct cells (36–38). Recently, Mall *et al.* (39) reported that β- rather than α- (δ-) ENaC is a rate-limiting element for salt absorption via airway epithelia. Absence of the essential β-subunit and weakly expression of the splicing variant δ-ENaC in CFPAC and Coca-2 cells may cause undetectable electrical activity (Fig. 1) (36). The possible physiologic function of ENaC, therefore, in pancreatic epithelial cells remains obscure.

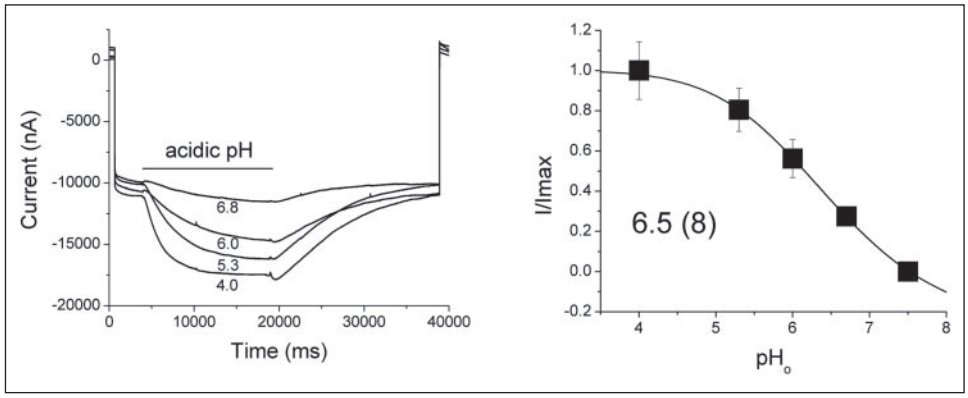

FIGURE 7. **Proton-activation of δαβγ-hENaC.** *A*, representative current traces activated by a drop in extracellular pH. Oocytes were held at 0 mV and stepped to −60 mV while acidic bath solutions were applied. *B*, dose response curve for proton-activation. The value of EC_{50} for proton activation is pH 6.5 ± 0.1, n = 8, which is greater than that of δβγ-hENaC (pH 6.1, $p < 0.05$) (25).

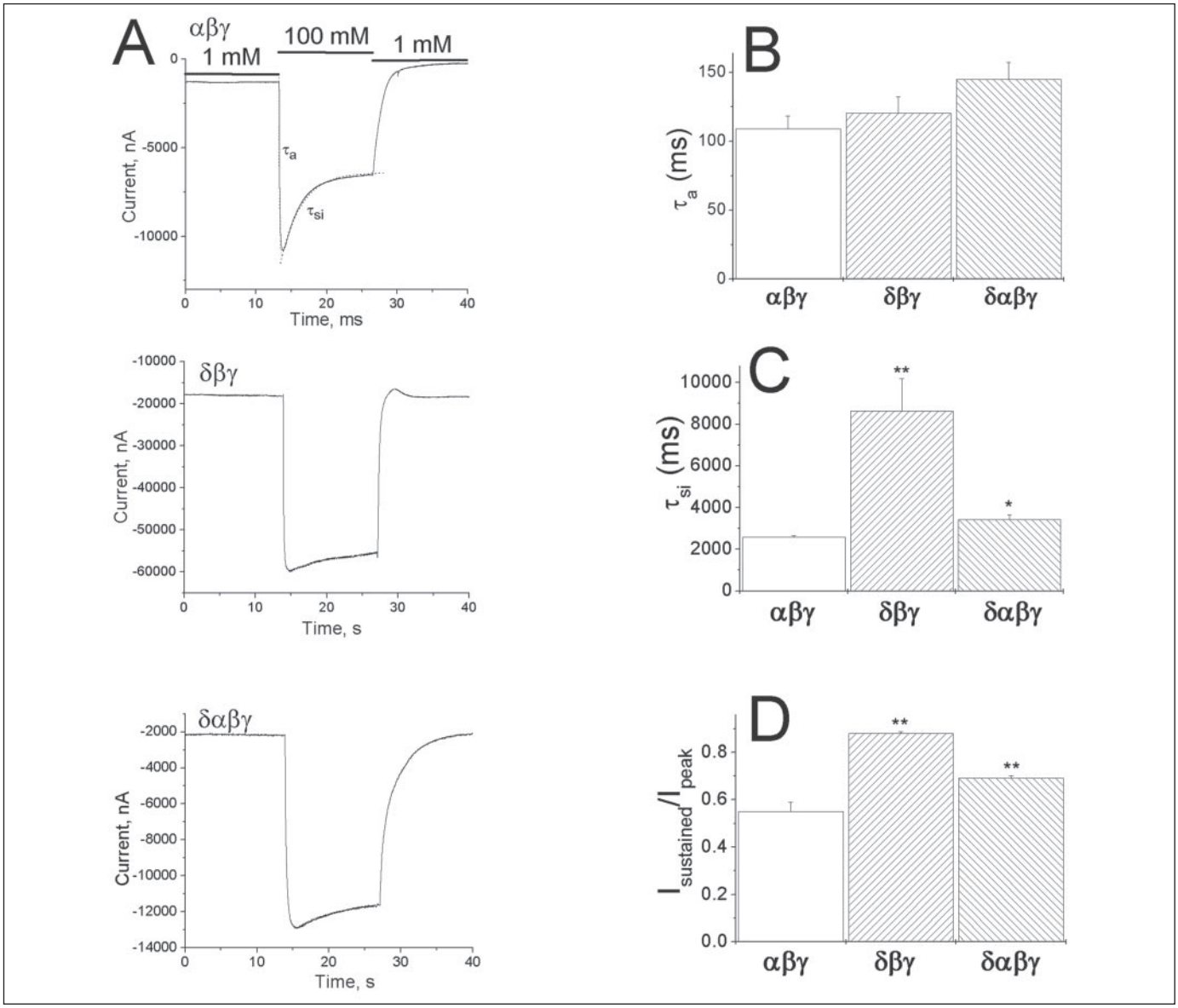

FIGURE 8. **Self-inhibition of δαβγ-ENaC.** Activation time (τ_a) and self-inhibition time (τ_{si}) were measured by fitting the current traces recorded while switching bath solution from low Na^+ ND-96 with 1 mM to regular ND-96 with 98.5 mM Na^+. *A*, representative current traces of αβγ- (*top*), δβγ- (*middle*), and δαβγ-ENaC (*bottom*) at −60 mV. To illustrate the fitting curves, *red* and *black dotted lines* created by fitting the current traces of αβγ-ENaC with the first order exponential function for τ_a and τ_{si}, respectively, were overlapped on the fitting regions. *B*, average activation time constants for αβγ- ($n = 42$), δβγ- ($n = 23$), and δαβγ-ENaC ($n = 13$). *C*, summary of self-inhibition time constants. *D*, current ratio of the sustained and peak currents ($I_{sustained}/I_{peak}$). *, $p < 0.05$, **, $p < 0.01$ when compared with αβγ-ENaC.

Increasing evidence indicates that the ion selectivity of native amiloride-sensitive channels is influenced by culture conditions and steroids (16, 18, 40). Stimulation of ENaC expression by hormones shows both subunit and tissue variability (2, 6, 28). However, in the present study, neither epithelial cells nor oocytes were treated with steroid hormones, and the epithelial cell lines for RT-PCR analysis were not grown on permeable supports. Subunit composition, but not subunit ratio, is a determinant of ENaC properties. αβ-ENaC possesses a high Na^+ permeability (P_{Na}/P_{Li}, = 1.2), unitary Na^+ conductance (5.1 pS), and K_i (4 μM) for amiloride (14, 15). In contrast to αβ-ENaC, δαβγ-hENaC has a much lower Na^+ permeability (P_{Na}/P_{Li}, 0.88), a distinctly different single channel Na^+ conductance (8 pS), and a K_i for amiloride (1.0 μM) (14, 15). Additionally, whole-cell amiloride-sensitive currents of αβ-, αγ-, δαβ-, and δαγ-hENaC channels were approximately −500 nA, which was only ~10% of that in oocytes expressing δαβγ-hENaC (data not shown). Our results ruled out the possibility that co-injection of δ- with αβγ-ENaC results in the formation of αβ-, αγ-, δαβ-, and δαγ-ENaC channels.

To address the question whether Ca^{2+} and Mg^{2+} can be transported by ENaC, we substituted Na^+ with equamolar Ca^{2+} or Mg^{2+} in the bath solution. Surprisingly, amiloride-sensitive Ca^{2+} and Mg^{2+} currents at hyperpolarization potentials were even greater than that carried by K^+. Our observations suggest that ENaC is permeable to divalent cations. The physiological impact of Ca^{2+} and Mg^{2+} permeability is unknown because the normal extracellular concentration for Ca^{2+} and Mg^{2+} is a few micromoles. Assuming that Ca^{2+} and Mg^{2+} competitively bind to the channel pore, the driving force would be too weak for Ca^{2+} and Mg^{2+} under physiologic conditions in which sodium is the predominant salt.

A question arising from our observations is whether there are two populations (*i.e.* αβγ- and δβγ-ENaC) or one population (δαβγ-ENaC) of ENaC. The ion selectivity and amiloride sensitivity of δαβγ-ENaC

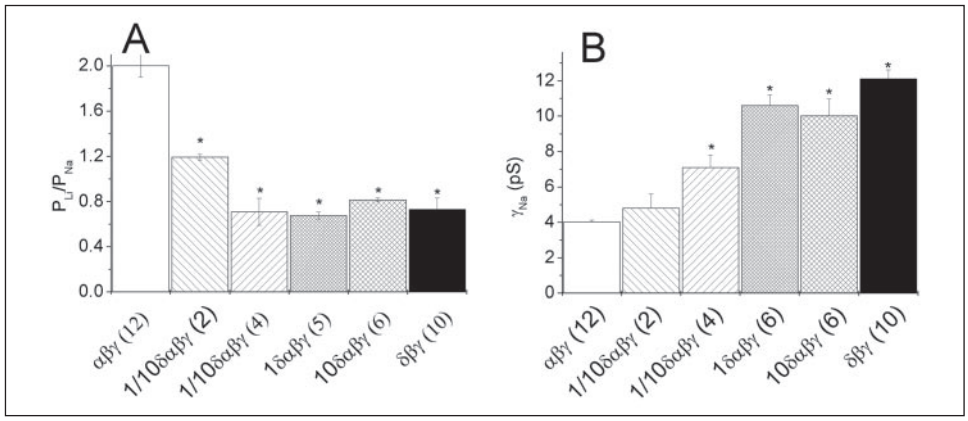

FIGURE 9. **cRNA concentration dependence of P_{Na}/P_{Li} ratio and unitary Na^+ conductance of δαβγ-ENaC.** *A*, P_{Na}/P_{Li} ratio examined under bi-ionic conditions. *B*, unitary Na^+ conductance for the corresponding groups. The ratios of δ/α subunit co-injected into three groups of oocytes were 1:10 (1/10δαβγ), 1:1 (aδαβγ), and 10:1 (10δαβγ). Two populations were observed in the first group of oocytes (1/10δαβγ); the permeability ratio and unitary conductance, therefore, were computed separately. *Numbers in brackets* are patches/oocytes measured. *, $p < 0.05$ when compared with αβγ-ENaC.

showed a mixture of those of αβγ- and δβγ-ENaC channels. Based on the assumption that there are two separate ENaC channels with distinguishable intrinsic features, two unitary Na^+ conductances should be detected in single channel experiments. However, only one Na^+ conductance of 8 pS, which is the arithmetic mean of αβγ- and δβγ-ENaC, was recorded. Moreover, analysis of the gating kinetics should demonstrate that the MOT value should be an average of αβγ- or δβγ-ENaC or should not differ from either one. However, the MOT value of δαβγ-ENaC is markedly less than both.

It is unlikely that either αβγ- or δβγ-ENaC is predominately expressed in oocytes due to the competitive exclusion between the two conducting subunits, α- and δ-ENaC. In addition to ion selectivity and amiloride sensitivity, the EC_{50} of the external pH for proton activation differs from that of δβγ-ENaC (25). αβγ-ENaC expressed in oocytes is not activated by extraoocyte acidosis (25). Furthermore, the self-inhibition experiments are not supportive of either αβγ- or δβγ-ENaC channels being expressed. The self-inhibition time and ratio of the sustained and peak currents are significantly greater than those of αβγ- but less than those of δβγ-ENaC.

Heterologously expressed δαβγ-ENaC has a unitary Na^+ conductance differing from those expressed in A549 cells (8 pS *versus* 4 and 20 pS) (6). The single channel Li^+ conductance of δαβγ-ENaC diverges from that in H441 cells (7 *versus* 11 pS) (2). It is not surprising to see differences in the biophysical characteristics between heterologously expressed δαβγ-ENaC and the native amiloride-sensitive Na^+ conductances in H441 and A549 cells. H441 cells only express a splicing variant of δ-ENaC (Fig. 1), the biophysical properties of which have not been characterized, and may contribute to these differences. Although we did not examine changes in unitary Li^+ conductance in oocytes expressing various ratios of variant δ- and α-ENaC, channels composed of the splicing variant may have a similar Li^+ conductance to that in H441 cells. On the other hand, culture conditions influence the biophysical properties and expression level of individual ENaC subunits (16, 18, 40). As our results show, the expression ratio between ENaC subunits governs the single channel features (Fig. 9). In addition, unknown ENaC subunits that have not been cloned or the splicing variants of δ-, α-, β-, γ-ENaC subunits as well as other amiloride-sensitive cation channels expressed in epithelial cells, for example, cyclic nucleotide-gated Na^+ channels, may contribute to the discrepancy between cloned ENaC and native epithelial Na^+ channels. Even for heterologously expressed αβγ-ENaC, the absence of cyclic AMP sensitivity and the differences in their whole-cell and single channel properties, when compared with the variety of amiloride-sensitive Na^+ channels expressed in number of native epithelia, are still unsolved questions. Therefore, δ-ENaC co-expression may contribute at least in part to the diverse properties of native epithelial Na^+ channels. Genetic manipulation of δ-ENaC expression, such as small interfering RNA, is required to further verify the contribution of δ-ENaC to native Na^+ transport across epithelia.

Our immunocytochemical results combined with the RT-PCR data demonstrate that δ-ENaC is co-expressed with α-, β-, and γ-ENaC in human pulmonary epithelial cells (Figs. 1–3). The question raised from these results is what level of δ-ENaC expression is required to alter the biophysical properties of αβγ-ENaC? Our results from heterologous co-expression of ENaC subunits in oocytes supported the notion that only a small amount of δ- may significantly impact on αβγ-ENaC properties. Existence of two subpopulations in oocytes co-injected 1δ:10α ENaC cRNAs indicated that they may have variable subunit composition. At present, the stoichiometry of δαβγ-ENaC is unknown.

The subunit-subunit interactions among α-, β-, and γ-ENaC have been demonstrated electrophysiologically using the two-electrode voltage clamp and patch clamp techniques and biochemically using co-immunoprecipitation and fluorescence resonance energy transfer (15, 41–45). In the present study, δ-ENaC immunoprecipitated with α- and γ-ENaC in H441 cells. In addition to the unique properties associated with δαβγ-ENaC, protein-protein interactions between δ- and α- or γ-ENaC supported the hypothesis that δ-ENaC may form multimeric channel complexes with the other ENaC orthologs. The δ-subunit contributes to the formation of the channel gate(s) and selective filter based on its involvement in amiloride sensitivity, cation selectivity, single channel conductance, gating pattern, and regulation by external protons and sodium (Figs. 3–8). Although we could not detect a possible interaction between native δ- and β-ENaC in H441 cells due to lack of a specific antibody for co-immunoprecipitation, previous studies have shown that tagged β-ENaC can co-immunoprecipitate with tagged α- and γ-ENaC (15, 41–45). Therefore, δ-ENaC may form channel complex with β-ENaC subunit by either direct or indirect associating with α- and γ-ENaC subunits.

These data indicated that δ-subunit can form a novel heteromultimeric channel complex with αβγ-ENaC in the oocyte expression system. The biophysical and pharmacological properties of δαβγ-ENaC differed from those of either αβγ-ENaC or δβγ-ENaC. The biophysical features of channels composed of δαβγ-ENaC offer a novel explanation for the differences observed in native amiloride-sensitive Na^+ conductances.

Acknowledgments—We greatly appreciate the gift of human δ-ENaC cDNA from Dr. Michel Lazdunski (Institut de Pharmacologie Moleculaire et Cellulaire, Valbonne, France), αβγ-hENaC clones from Dr. Michael J. Welsh (University of Iowa), and HA-tagged δ-construct from Dr. Fiona J McDonald (University of Otago, New Zealand). We acknowledge Mei-Qin Zeng, Susan J. Anderson, Melissa McCarthy, and Glenda Davis for technical assistance.

REFERENCES

1. Garty, H., and Palmer, L. G. (1997) *Physiol. Rev.* **77,** 359–396
2. Itani, O. A., Auerbach, S. D., Husted, R. F., Volk, K. A., Ageloff, S., Knepper, M. A., Stokes, J. B., and Thomas, C. P. (2002) *Am. J. Physiol.* **282,** L631–L641
3. Lazrak, A., and Matalon, S. (2003) *Am. J. Physiol.* **285,** L443–L450
4. Benos, D. J., Awayda, M. S., Berdiev, B. K., Bradford, A. L., Fuller, C. M., Senyk, O., and Ismailov, II (1996) *Kidney Int.* **49,** 1632–1637
5. Matalon, S., and O'Brodovich, H. (1999) *Annu. Rev. Physiol.* **61,** 627–661
6. Lazrak, A., Samanta, A., and Matalon, S. (2000) *Am. J. Physiol.* **278,** L848–L857
7. Kellenberger, S., and Schild, L. (2002) *Physiol. Rev.* **82,** 735–767
8. Canessa, C. M., Schild, L., Buell, G., Thorens, B., Gautschi, I., Horisberger, J. D., and Rossier, B. C. (1994) *Nature* **367,** 463–467
9. Waldmann, R., Champigny, G., Bassilana, F., Voilley, N., and Lazdunski, M. (1995) *J. Biol. Chem.* **270,** 27411–27414
10. McDonald, F. J., Snyder, P. M., McCray, P. B., Jr., and Welsh, M. J. (1994) *Am. J. Physiol.* **266,** L728–L734
11. Babini, E., Geisler, H. S., Siba, M., and Grunder, S. (2003) *J. Biol. Chem.* **278,** 28418–28426
12. Canessa, C. M., Horisberger, J. D., and Rossier, B. C. (1993) *Nature* **361,** 467–470
13. Lingueglia, E., Voilley, N., Waldmann, R., Lazdunski, M., and Barbry, P. (1993) *FEBS Lett.* **318,** 95–99
14. McNicholas, C. M., and Canessa, C. M. (1997) *J. Gen. Physiol.* **109,** 681–692
15. Fyfe, G. K., and Canessa, C. M. (1998) *J. Gen. Physiol.* **112,** 423–432
16. Yue, G., Hu, P., Oh, Y., Jilling, T., Shoemaker, R. L., Benos, D. J., Cragoe, E. J., Jr., and Matalon, S. (1993) *Am. J. Physiol.* **265,** C630–C640
17. Jain, L., Chen, X. J., Ramosevac, S., Brown, L. A., and Eaton, D. C. (2001) *Am. J. Physiol.* **280,** L646–L658
18. Hamilton, K. L., and Eaton, D. C. (1985) *Am. J. Physiol.* **249,** C200–C207
19. Staruschenko, A., Medina, J. L., Patel, P., Shapiro, M. S., Booth, R. E., and Stockand, J. D. (2004) *J. Biol. Chem.* **279,** 27729–27734
20. Ji, H. L., Parker, S., Langloh, A. L., Fuller, C. M., and Benos, D. J. (2001) *Am. J. Physiol.* **281,** C64–C74
21. Ji, H. L., Bishop, L. R., Anderson, S. J., Fuller, C. M., and Benos, D. J. (2004) *J. Biol. Chem.* **279,** 8428–8440
22. Fu, J., Ji, H. L., Naren, A. P., and Kirk, K. L. (2001) *J. Physiol.* (*Lond.*) **536,** 459–470
23. Becchetti, A., Malik, B., Yue, G., Duchatelle, P., Al-Khalili, O., Kleyman, T. R., and Eaton, D. C. (2002) *Am. J. Physiol.* **283,** F1030–F1045
24. Wodopia, R., Ko, H. S., Billian, J., Wiesner, R., Bartsch, P., and Mairbaurl, H. (2000) *Am. J. Physiol.* **279,** L1110–L1119
25. Ji, H. L., and Benos, D. J. (2004) *J. Biol. Chem.* **279,** 26939–26947
26. Sheng, S., Bruns, J. B., and Kleyman, T. R. (2004) *J. Biol. Chem.* **279,** 9743–9749
27. Chraibi, A., and Horisberger, J. D. (2002) *J. Gen. Physiol.* **120,** 133–145
28. Ramminger, S. J., Richard, K., Inglis, S. K., Land, S. C., Olver, R. E., and Wilson, S. M. (2004) *Am. J. Physiol.* **287,** L411–L419
29. Sayegh, R., Auerbach, S. D., Li, X., Loftus, R. W., Husted, R. F., Stokes, J. B., and Thomas, C. P. (1999) *J. Biol. Chem.* **274,** 12431–12437
30. Tucker, J. K., Tamba, K., Lee, Y. J., Shen, L. L., Warnock, D. G., and Oh, Y. (1998) *Am. J. Physiol.* **274,** C1081–C1089
31. Lazrak, A., Samanta, A., Venetsanou, K., Barbry, P., and Matalon, S. (2000) *Am. J. Physiol.* **279,** C762–C770
32. Clunes, M. T., Butt, A. G., and Wilson, S. M. (2004) *J. Physiol.* (*Lond.*) **557,** 809–819
33. Hardiman, K. M., McNicholas-Bevensee, C. M., Fortenberry, J., Myles, C. T., Malik, B., Eaton, D. C., and Matalon, S. (2004) *Am. J. Respir. Cell Mol. Biol.* **30,** 720–728
34. Fukuda, M., Ohara, A., Bamba, T., and Saek, Y. (2000) *Jpn. J. Physiol.* **50,** 215–225
35. Bremner, H. R., Freywald, T., O'Brodovich, H. M., and Otulakowski, G. (2002) *Am. J. Physiol.* **282,** L124–L134
36. Novak, I., and Hansen, M. R. (2002) *Biochim. Biophys. Acta* **1566,** 162–168
37. Zhao, W. C., Zhu, J. X., Tang, N., Gou, Y. L., Rowlands, D. K., Chung, Y. W., Xing, Y., and Chan, H. C. (2003) *World J. Gastroenterol.* **9,** 2505–2508
38. Cotton, C. U. (1998) *Pancreas* **17,** 247–255
39. Mall, M., Grubb, B. R., Harkema, J. R., O'Neal, W. K., and Boucher, R. C. (2004) *Nat. Med.* **10,** 487–493
40. Jain, L., Chen, X. J., Malik, B., Al-Khalili, O., and Eaton, D. C. (1999) *Am. J. Physiol.* **276,** L1046–L1051
41. Kosari, F., Sheng, S., Li, J., Mak, D. O., Foskett, J. K., and Kleyman, T. R. (1998) *J. Biol. Chem.* **273,** 13469–13474
42. Staruschenko, A., Adams, E., Booth, R. E., and Stockand, J. D. (2005) *Biophys. J.* **88,** 3966–3975
43. Berdiev, B. K., Jovov, B., Tucker, W. C., Naren, A. P., Fuller, C. M., Chapman, E. R., and Benos, D. J. (2004) *Am. J. Physiol.* **286,** F1100–F1106
44. Prince, L. S., and Welsh, M. J. (1998) *Biochem. J.* **336,** 705–710
45. Biasio, W., Chang, T., McIntosh, C. J., and McDonald, F. J. (2004) *J. Biol. Chem.* **279,** 5429–5434